Conductance Enhancement of Nano-Particulate Indium Tin Oxide Layers Fabricated by Printing Technique

M. Gross, I. Maksimenko, H. Faber, N. Linse, P. J. Wellmann

University of Erlangen-Nuremberg, Materials Department 6, Martensstr. 7, 91058 Erlangen, Germany

ABSTRACT

To improve the conductance of nano particulate indium tin oxide (In_2O_3:Sn, ITO) layers we have applied a number of treatments: post bake, infiltration by an ITO precursor solution with subsequent sol-gel transformation into ITO, treatment with etching agents as well as annealing in vacuum. We obtained a maximum conductance of 120 $\Omega^{-1}cm^{-1}$ by combining the precursor infiltration technique with vacuum annealing. Considering the layer thickness of 5.2 µm, this value corresponds to a sheet resistance of about 16 Ω/□ at a maximum transmittance of 83 %. These nano particulate layers should be applicable as electrodes in optoelectronics.

To understand the mechanisms behind the conductance improvement and to fathom the limits we did some investigations: long-term resistance measurements gave an insight in oxygen vacancy balance concentration. From infrared absorption measurements we inferred the free charge carrier density and at present we carry out XPS measurements which yield information about the alteration of oxygen vacancy concentration. Considering these data we discuss two conductance improving mechanisms: The increase of the free charge carrier density by a rise of oxygen vacancy concentration as well as a release of trapped charge carriers from the aggregate surfaces.

Keywords: ITO, nanoparticles, transmittance, conductance

1 INTRODUCTION

Indium tin oxide (ITO, In_2O_3:SnO_2) thin films exhibit a high conductance at coexistent brilliant transparency [66Gro,83Ray,86Ham]. Therefore ITO is widely-used as transparent electrode material in optoelectronic applications as TFT-LCD-s [99Kat,07Gai], touch screens, organic light emitting diodes [07Gär], organic solar cells [04Bra,06Wal] and electro-chromic devices [06Gra]. The state-of-the-art ITO layer fabrication techniques are physical vapour deposition methods (especially sputtering) [83Ray,03Fra], laser deposition [01Suz] or evaporation [93Rau,01Bae]. Typical for these layers are conductance values of more than 10,000 $\Omega^{-1}cm^{-1}$ [93Rau,01Suz]. As drawback, the great values demand cost intensive vacuum processes as well as patterning by an additional etching step [99Kat] which involves a strong material loss. Indium tin oxide layers deposited from nanoparticle dispersions are of emerging interest due to the printability which comes along with large area fabrication potential as well as direct patterning possibility [06Ald,07Gro]. Nano particulate layers exhibit comparatively low conductance [06Ald,07Gro,03Ede] which hitherto impeded their use in modern optoelectronic applications despite their advantages of low production costs and a significant lower absorption coefficient.

In a previous work we found a conductance increase from 0.018 $\Omega^{-1}cm^{-1}$ to 17 $\Omega^{-1}cm^{-1}$ by using a temperature treatment in air at 550°C [07Gro]. Here we present further post annealing treatments: post bake, infiltration by an ITO precursor solution with subsequent sol-gel transformation into ITO, treatment with etching agents as well as annealing in vacuum.

2 EXPERIMENTAL

We fabricated nano particulate ITO layers by spin-coating a commercially available (Evonik Degussa GmbH) ethanolic dispersion with a Headway EC101 spin coater on 20 mm × 20 mm × 0.14 mm glass substrates with subsequent annealing at 550°C for 30 min in air. This leads to approx. 1000 nm thick layers which are the initial samples for all following treatments:

Post bake treatment means a temperature step at 250°C for 5 min in air.

Infiltration treatment was done by dipping the samples for 15 s in an ITO precursor solution which was prepared following the recipe of Daoudi et al. [03Dao]. Afterwards the precursor gelification was carried out by drying the samples at 150°C for 30 min. Transformation into ITO however takes place during subsequent annealing at 550°C for 30 min in air.

Etching treatment was carried out by dipping the samples in aqueous 1 M HCl solution for 15 s and washing with water.

Vacuum annealing means temperature treatment in a fused silica tube at 550°C for 30 min at a pressure of about 10^{-5} mbar.

We characterised the nano particulate ITO layers with a number of techniques: Sheet resistance measurements in a linear four-probe setup using a Keithley SMU 236. Layer thickness was determined with a DekTak IIA mechanical profilometer. High resolution SEM (Hitachi S4800) visualised the layer morphology and porosity which itself was calculated via refractive index calculation using the method of Manifacier et al. [76Man,07Gro]. The required transmittance spectra were measured with a Perkin Elmer

NSTI-Nanotech 2008, www.nsti.org, ISBN 978-1-4200-8503-7 Vol. 1

Lambda 19 spectrometer. There from we also deduced the free charge carrier concentration.

3 RESULTS AND DISCUSSION

As deposited layer conductance is only 0.018 $\Omega^{-1}cm^{-1}$, but it can be increased by annealing in air at 550°C to 5.7 $\Omega^{-1}cm^{-1}$. In Fig. 1 we present an overall view how several additional post annealing treatments impact the layer conductance.

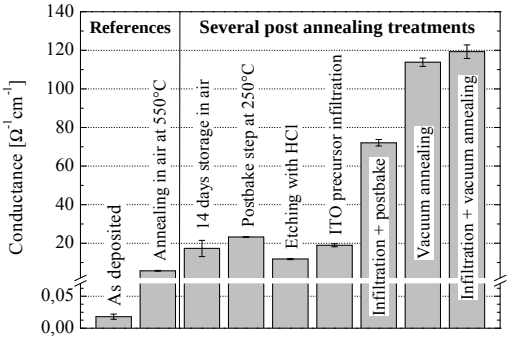

Fig. 1: Impact of several post annealing treatments on conductance of printed nano particulate ITO layers

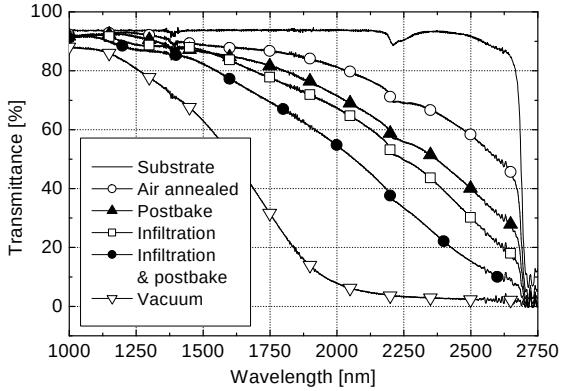

Fig. 2: Near-IR transmittance spectra of various treated ITO layers. The shift of the plasma absorption edge towards shorter wavelength indicates an increase in free charge carrier concentration [86Ham]

3.1 Post bake treatment

We found that the layer conductance increases with storage time after annealing at 550°C in air up to a saturation level (see Fig. 3). A 14 days storage in environment for example leads to a conductance of 17,4 $\Omega^{-1}cm^{-1}$, storage in dry air to 21.1 $\Omega^{-1}cm^{-1}$. This effect was also reported by Ederth et al. [02Ede]. As presented in Table 1 we found 250°C as the optimum post bake temperature. This post bake treatment for only 5 min leads to a conductance increase to 23.2 $\Omega^{-1}cm^{-1}$ which is comparable to the conductance after storage.

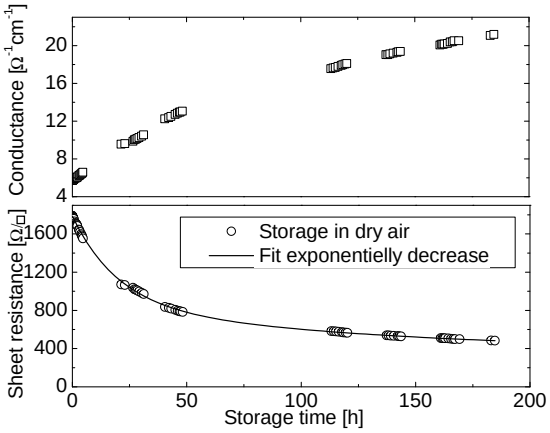

Fig. 3: Conductance and sheet resistance of annealed samples with storage time in dry air

Post bake temperature	20	100	150	200
Sheet resistance [Ω/□]	2956	2446	1275	967
Post bake temperature	250	300	400	500
Sheet resistance [Ω/□]	743	856	1272	2010

Table 1: Sheet resistance versus post bake temperature

The mechanism behind the conductance increase after sample storage, as well after post bake treatment is not fully understood. The phenomenon can be attributed either (i) to an acceleration of the kinetic of oxygen diffusion out of the ITO material or (ii) to modification of surface band bending. The oxygen vacancy balance concentration in the ITO particle interior at the annealing temperature of 550°C should not significantly change after heat treatment. Therefore, the conductivity increase after storage of the samples for 14 days or post bake at 250°C is most likely related to a change of surface band bending with a resulting greater surface conductivity due to an increased charge carrier concentration. Beside surface band bending, enhanced oxygen diffusion along grain boundaries in the nano particulate layers may impact oxygen vacancy and, hence, charge carrier concentration, at grain boundaries within the nano-particulate system. The latter is supported by the date in Fig. 2, that indicate a shift of the plasma edge towards shorter wavelength (see also [86Ham, 03Ald]).

3.2 Infiltration treatment

After nanoparticle dispersion deposition and annealing step the ITO layers exhibit a porosity of more than 40 % [07Gro]. The aim of infiltration experiments first was to decrease the porosity and to increase the contact area between the nanoparticle aggregates by bringing in additional ITO material.

Thereby we found that there is no impact if the layers are infiltrated in vacuum or in air. If the samples stand in a

puddle of precursor solution the rising infiltration edge can be observed demonstrating that infiltration really takes place. More homogeneous results however are obtained by dipping the samples into the precursor solution for about 15 s and subsequent spinning away the surplus solution.

Precursor infiltration into the layers and subsequent transformation to ITO leads to an increased layer conductance of 19.0 $\Omega^{-1}cm^{-1}$ (Fig. 1) due to an increase in free charge carrier concentration (plasma edge shift in Fig. 2).

By the combination of infiltration and post bake treatment a significant higher conductance of 72.1 $\Omega^{-1}cm^{-1}$ is achieved (Fig. 1). Thereby the plasma edge shift is larger in comparison to that of both single treatments. This indicates the presence of a second mechanism of charge carrier increase:

At the surface of the nanoparticle aggregates probably exists a depletion layer due to charge carrier trapping in surface defect states and by surface band bending. We now suggest that the precursor solution dissolves this depletion layer and probably partially replaces it with a new generated undepleted sol-gel ITO layer.

This thesis is supported by some results: On the one hand we found no significant conductance increase after multiple infiltration steps and on the other hand we unexpectedly obtained no porosity decrease too. It is rather a slight increase (see Table 2). Multiple infiltration hereby means a repetition of the sequence: precursor infiltration, gelification and precursor transformation.

Infiltration steps	0	1	2	3	4	5
Porosity [%]	42.4	43.2	43.7	43.7	44.0	43.8

Table 2: ITO layer porosity after some infiltration steps

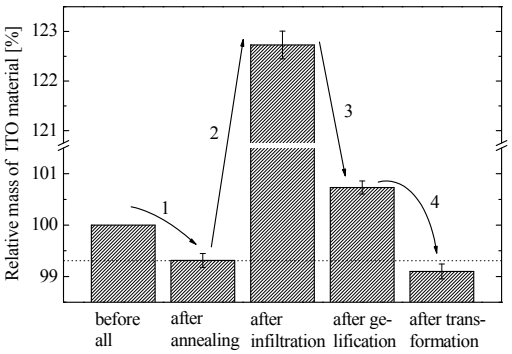

Fig. 4: Relative mass of ITO pellets along the infiltration process sequence

To verify this porosity results we measured the mass of ITO pellets along the infiltration process sequence. We used pellets because of the poor ITO to substrate mass ratio in the case of standard thin film samples. The relative masses are presented in Fig. 4. The mass decrease from green body to annealed pellet (1) presumably dues to evaporation of adsorbed species from surface. The infiltration step itself leads to a significant mass increase (2) due to the additional mass of precursor solution solvent in the pores. The gelification (3) is connected with the loss of this solvent mass. Only the mass of ITO precursor molecules remains. These molecules (indium chelate complex ions) [03Dao] are disturbed during transformation at 550°C and all organic is burned out (4). The complete infiltration and transformation process is connected with a slight mass loss which verifies the found minor porosity increase.

These results as well as the deed that etching of ITO layers in 1 M HCl acid also leads to a conductance increase (see Fig. 1, details will be presented elsewhere) affirms the hypothesis of dissolving respectively etching of a surface depletion layer by the precursor solution and refutes the first assumption of partially fulfilling of the pores with sol-gel ITO material.

3.3 Vacuum infiltration

It is noteworthy that conductance enhancement by infiltration and post bake is long-term stable and the achieved ITO layers are still in the oxidised yellowish state indicating a relative low charge carrier concentration. It is well known that temperature treatment of ITO layers in vacuum or reducing atmospheres leads to a further conductance increases since oxygen diffuses out which increases oxygen vacancy concentration and with it the charge carrier density [02Ede,03Ald]. Thereby the ITO is transformed to the reduced bluish state.

We observed conductances up to 113.8 $\Omega^{-1}cm^{-1}$ (Fig. 1) after annealing at 550°C at a pressure of about 10^{-5} mbar, whereas the achieved conductance strongly depends on the vacuum quality.

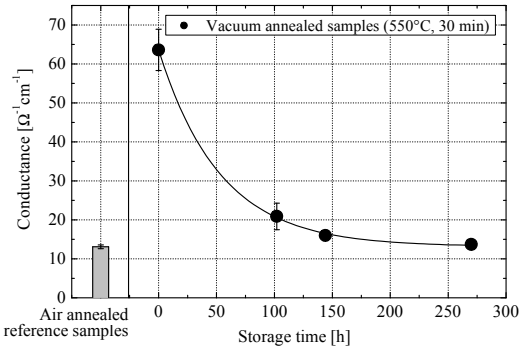

Fig. 5: Time dependent conductance of vacuum annealed nanoparticulate ITO layers

With increasing storage time in air the conductance is declining due to back-diffusion of oxygen (see at Fig. 5). The significant increase in free charge carrier concentration appears in the strong plasma edge shift towards shorter wavelength (Fig. 2) and the widening of the optical band gap due to Burstein-Moss-effect (Fig. 6).

NSTI-Nanotech 2008, www.nsti.org, ISBN 978-1-4200-8503-7 Vol. 1

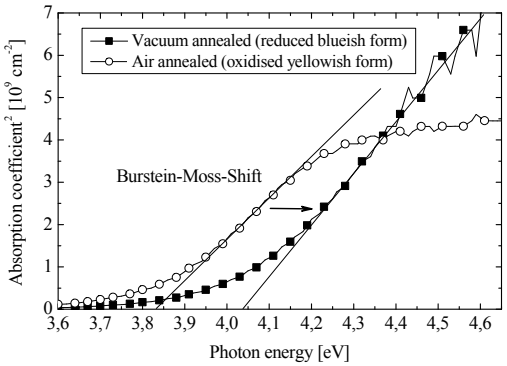

Fig. 6: Widening of the optical bandgap after vacuum annealing due to Burstein-Moss-effect

3.4 Best conductance

By combining infiltration treatment and vacuum annealing we obtained a maximum conductance of 119.3 Ω^{-1}cm^{-1} which represents a slight increase compared to single vacuum annealing. A possible reason is the additional release of charge carriers from surface trap states as discussed above, whereas the mechanism of charge carrier generation by vacuum annealing does not impact these trapped electrons. But as mentioned above, the achieved conductance by vacuum annealing strongly depends on the experimental conditions. Therefore this slight increase perhaps can have other reasons.

However, infiltrated and vacuum annealed nanoparticulate layers exhibit a conductance high enough to be applicable in modern optoelectronics. For example we achieved layers with a sheet resistance of 17 Ω/□ at a coexistent transmittance through the complete stack of glass substrate and ITO layer of more than 80 %. The latter may be applied to organic light emitting device processing.

4 OUTLOOK

At present we carry out XPS (ESCA) measurements of variously treated ITO layers to clarify the mechanisms behind the conductance increase: The oxygen O^{2-}:1s ESCA peak of ITO typically has a small shoulder and can be separated into two super-positioning single peaks O^{2-}_{I}:1s at binding energies in the range of 531.2 … 531.6 eV and O^{2-}_{II}:1s at about 529.9 eV. The first peak is generated by O^{2-}-ions from oxygen-deficient regions, whereas the second one belongs to O^{2-}-ions having neighbouring In atoms with their full complement of six nearest neighbouring O^{2-}-ions [77Fan]. The O^{2-}_{I}:1s / O^{2-}_{II}:1s-ratio therefore should be a direct indicator for the number of oxygen vacancies in the material. By combining these results with optical measurements of plasma edge we hopefully are able to clearly separate both mechanisms: charge carrier density increase by rising oxygen vacancy concentration on the one hand and by release of trapped carriers on the other hand.

ACKNOWLEDGEMENT

This work is financially supported by DFG (contract number GRK 1161) and Evonik Degussa GmbH. Fruitful discussions with Dr. Dieter Adam and Dr. Anna Prodi-Schwab from Evonik Degussa GmbH, Creavis Technologies and Innovation are gratefully acknowledged.

REFERENCES

[66Gro] R. Groth, Phys. Stat. Sol. 14 (1966) 69

[83Ray] S. Ray, R. Banerjee, N. Basu, A.K. Batabyal, A.K. Barua, J. Appl. Phys 54 (1983) 3497

[86Ham] I. Hamberg, C.G. Granqvist, J. Appl. Phys. 60(11) (1986) R123

[99Kat] M. Katayama, Thin Solid Films, 341 (1999) 140

[07Gai] M. Gaillet, L. Yan, E. Teboul, Thin solid films, *in press 2007*

[07Gär] C. Gärditz, A. Winnacker, F. Schindler, R. Paetzold, Appl. Phys. Lett. 90 (2007) 103506

[04Bra] C.J. Brabec, Sol. Energ. Mat. Sol. C. 83 (2004) 273

[06Wal] C. Waldauf, M.C. Scharber, P. Schilinsky, J.A. Hauch, C.J. Brabec, J. Appl. Phys 99 (2006) 104503

[06Gra] C.G. Granqvist, Nat. Mater. 5 (2006) 89

[03Fra] P. Frach, D. Glöß, K. Goedicke, M. Fahland, W.M. Gnehr, Thin Solid Films 445 (2003) 251

[01Suz] A. Suzuki, T. Matsushita, T. Aoki, Y. Yoneyama, M. Okuda, Jpn. J. Appl. Phys. 40 (2001) L401

[93Rau] I.A. Rauff, Mater. Lett. 18(3) (1993) 123

[01Bae] J.W. Bae, J.S. Kim, G.Y. Yeom, Nucl. Iinstrum. Meth. B 178 (2001) 311

[06Ald] N. Al-Dahoudi, M.A. Aegerter, Thin Solid Films, 502 (2006) 193

[07Gro] M. Gross, A. Winnacker, P.J. Wellmann, Thin Solid Films 515 (2007) 8567

[03Ede] J. Ederth, P. Heszler, A. Hultåker, G.A. Niklasson, C.G. Granqvist, Thin Solid Films, 445 (2003) 199

[03Dao] K. Daoudi, B. Canut, M.G. Blanchin, C.S. Sandu, V.S. Teodorescu, J.A. Roger, Thin Solid Films 445 (2003) 20

[76Man] J.C. Manifacier, J. Gasiot, J.P. Fillard, J Phys E Sci Instrum 9 (1976) 1002

[02Ede] J. Ederth, A. Hultåker, P. Heszler, G.A. Niklasson, C.G. Granqvist, A.v. Doorn, C.v. Haag, M.J. Jongerius, D. Burgard, Smart Mater. Struct. 11 (2002) 675

[03Ald] N. Al-Dahoudi, PhD thesis, university of Saarland and INM (2003)

[77Fan] J.C.C. Fan, J.B. Goodenough, J. Appl. Phys. 48 (1977) 3524